John von Neumann Institute for Computing

Realistic Modeling of Materials with Strongly Correlated Electrons

Georg Keller, Karsten Held, Volker Eyert,
Vladimir I. Anisimov, Krysztof Byczuk, Markus Kollar,
Ivan Leonov, Xinguo Ren, and Dieter Vollhardt

published in

NIC Symposium 2006 ,
G. Münster, D. Wolf, M. Kremer (Editors),
John von Neumann Institute for Computing, Jülich,
NIC Series, Vol. **32**, ISBN 3-00-017351-X, pp. 183-190, 2006.

http://www.fz-juelich.de/nic-series/volume32

Realistic Modeling of Materials with Strongly Correlated Electrons

Georg Keller[1], Karsten Held[2], Volker Eyert[1], Vladimir I. Anisimov[3], Krzysztof Byczuk[1], Markus Kollar[1], Ivan Leonov[1], Xinguo Ren[1], and Dieter Vollhardt[1]

[1] Theoretical Physics III, Center for Electronic Correlations and Magnetism
Institute for Physics, University of Augsburg, 86135 Augsburg, Germany
E-mail: {Georg.Keller, Dieter.Vollhardt}@physik.uni-augsburg.de

[2] Max-Planck-Institut für Festkörperforschung, 70569 Stuttgart, Germany
[3] Institute of Metal Physics, S. Kovalevskoj Str. 18, Ekaterinburg GSP-170, 620219 Russia

1 Introduction

Modern solid state physics explains the physical properties of numerous materials such as simple metals, and some semiconductors and insulators. But materials with open d and f shells, where electrons occupy narrow orbitals, have properties that are harder to explain. In transition metals such as vanadium, iron and their oxides, for example, electrons experience strong Coulombic repulsion because of their spatial confinement in those orbitals. Such strongly interacting or "correlated" electrons cannot be described as embedded in a static mean field generated by the other electrons[1,2]. The d and f electrons have internal degrees of freedom (spin, charge, orbital moment) whose interplay leads to a whole "zoo" of exotic ordering phenomena at low temperatures. As a consequence, strongly correlated electron systems are extremely sensitive to small changes in their control parameters (temperature, pressure, doping, etc.), resulting in strongly nonlinear responses, and tendencies to phase separate or form complex patterns in chemically inhomogeneous situations. For this reason strongly correlated materials display dramatic effects which range from large changes of the resistivity across the metal-insulator transitions in V_2O_3, and considerable volume changes across phase transitions (volume collapse effect) in actinides and lanthanides, to exceptionally high transition temperatures (above liquid nitrogen temperatures) in superconductors with copper oxygen planes, and remarkable mass renormalizations in materials called heavy fermion systems which at low temperatures behave as free electrons with masses as large as a thousand times the mass of a free electron. Furthermore, some strongly correlated materials have a very large thermoelectric response. A great sensitivity of the resistivity to applied magnetic fields, dubbed colossal magnetoresistance was discovered recently and a gigantic nonlinear optical susceptibility with an ultrafast recovery time was discovered in Mott insulating chains. These properties make the prospects for applications of correlated materials exciting, and their theoretical and experimental study very challenging.

One especially striking correlation phenomenon is the phase transition between a paramagnetic metal and a paramagnetic insulator caused by the Coulomb interaction between the electrons which is referred to as Mott-Hubbard metal-insulator transition[1–3]. Reliable

microscopic investigations of this many-body phenomenon are known to be exceedingly difficult. Indeed, the question concerning the nature of this transition poses one of the fundamental theoretical problems in condensed matter physics. Correlation-induced metal-insulator transitions (MIT) of this type are found, for example, in transition metal oxides with partially filled bands near the Fermi level. In these systems band theory typically predicts metallic behavior. The most famous example is V_2O_3 doped with Cr[4]. While at low temperatures V_2O_3 is an antiferromagnetic insulator (AFI) with monoclinic crystal symmetry, the high-temperature paramagnetic phase has a corundum structure. The MIT in the paramagnetic phase is iso-structural; only the ratio of the c/a axes changes discontinuously. This may be taken as an indication for a predominantly electronic origin of this transition.

The investigation of electronic many-particle systems is made especially complicated by quantum statistics, and by the fact that the phenomena of interest (e.g., metal-insulator transitions and magnetism) usually require the application of nonperturbative theoretical techniques. In the last decade, a new approach for treating electronic lattice models, the dynamical mean-field theory (DMFT), has led to new analytical and numerical opportunities to study correlated electronic systems[1,5]. This theory – initiated by Metzner and Vollhardt in 1989 – is exact in the limit of infinite dimensions ($d = \infty$)[6]. In this limit, the problem is reduced to a single-impurity Anderson model with self consistency condition[7,8], allowing for quantum Monte-Carlo (QMC) simulations without a sign problem for one-band models (for multi-band models, see Ref. 9), i.e., down to temperatures $T \sim 10^{-2}W$ where W is the bandwidth.

Recently, the LDA+DMFT, a new computation scheme that merges electronic band structure calculations and the dynamical mean field theory, was developed[1,10,11]. Starting from conventional band structure calculations in the local density approximation (LDA) the correlations are taken into account by a Hubbard interaction term and a Hund's rule coupling term. The resulting DMFT equations are solved numerically with a parallelized auxiliary-field quantum Monte-Carlo algorithm (QMC). In contrast to LDA or LDA+U the many-body scheme LDA+DMFT provides the correct physics for all Coulomb interactions and dopings. Namely, LDA yields an uncorrelated metal even if the material at hand is a strongly-correlated metal or a Mott insulator. Similarly, LDA+U yields an insulator for the *ab-initio*-calculated U-values of 3d transition metal oxides, even for materials which should be metallic.

So far the LDA+DMFT method is the most successful tool available to investigate correlation effects in transition metal oxides. Recent developments will allow us to apply the method to a wider range of systems. In most previous studies the LDA band structure served only as input information for the DMFT, but there was no feedback from DMFT to LDA. Since the DMFT result can in principle change the charge distribution on which the LDA band structure depends one should feed back the changes introduced by the DMFT into LDA and repeat the calculation until convergence is reached in both parts. This procedure is currently being investigated. Furthermore, calculations should not only include the orbitals of the correlated electrons, but *all* hybridizing orbitals. Such an extended computational scheme has recently been developed and applied in Wannier basis[12]. For crystal structures with strong hybridization and/or low symmetry it is also necessary to obtain the off-diagonal matrix elements of the local Green function from the QMC calculation. This extension is currently being tested and will be applied in our future computational

investigations of correlated materials.

In this paper we limit our discussion to the LDA+DMFT investigation of only one material, namely V_2O_3 in the paramagnetic insulating and metallic phase.

2 The LDA+DMFT Method

In a first step, the LDA band structure and the densities of states for the crystal structures of metallic V_2O_3 and insulating $(V_{0.962}Cr_{0.038})_2O_3$ are calculated. The LDA DOS for both materials are found to be metallic in contrast to experimental results. The reason for this failure is the fact that LDA deals with electronic correlations only very rudimentarily, namely, the dependence of the LDA exchange-correlation energy on the electron density is given by perturbative or quantum Monte-Carlo calculations for jellium[13], which is a weakly correlated system. To overcome this shortcoming, we supplement the LDA band structure by the the most important Coulomb interaction terms, i.e., the local Coulomb repulsion U and the local Hund's rule exchange J. The local Coulomb repulsion U gives rise to a genuine effect of electronic correlations, the Mott-Hubbard metal-insulator transition[1,5,14]. If the LDA bandwidth is considerably larger than the local Coulomb interaction, the LDA results are slightly modified but the system remains a metal. If the LDA bandwidth is much smaller than the local Coulomb interaction one essentially has the atomic problem where it costs an energy of about U to add an electron and the system is an insulator. In between the Mott-Hubbard metal-insulator transition occurs, with V_2O_3 being on the metallic side whereas $(V_{0.962}Cr_{0.038})_2O_3$, which has a 0.1-0.2 eV smaller bandwidth, is on the insulating side.

Interpreting the LDA band structure as resulting from a one-particle Hamiltonian $\hat{H}^0_{\mathrm{LDA}}$ and supplementing the latter with the local Coulomb interactions gives rise to the multi-band many-body Hamiltonian[10,15]

$$\hat{H} = \hat{H}^0_{\mathrm{LDA}} + U \sum_{i\ m} \hat{n}_{im\uparrow}\hat{n}_{im\downarrow} + \sum_{i\ m\neq\tilde{m}\ \sigma\tilde{\sigma}} (V - \delta_{\sigma\tilde{\sigma}} J)\ \hat{n}_{im\sigma}\hat{n}_{i\tilde{m}\tilde{\sigma}}. \quad (1)$$

Here, i denotes the lattice site and $\hat{n}_{im\sigma}$ is the operator for the occupation of the t_{2g} orbital m with spin $\sigma \in \{\uparrow, \downarrow\}$. The interaction parameters are related by $V = U - 2J$ which is a consequence of orbital rotational symmetry. This holds exactly for degenerate orbitals and is a good approximation for V_2O_3 where the t_{2g} bands have similar centers of gravity and bandwidths. As in the local spin density approximation (LSDA), the spin-flip term of the exchange interaction is not taken into account in Eq. (1). Furthermore, a pair hopping term proportional to J is neglected since it requires that one orbital is entirely empty while another is entirely full which is a rare situation and corresponds to highly excited states. For the Hund's rule coupling J we take the value $J = 0.93$ eV obtained from constrained LDA. By contrast, a reliable calculation of the Coulomb repulsion U is made difficult by the fact that U depends sensitively on screening, leading to uncertainties of about 0.5 eV[11]. For our present purposes this uncertainty is too large since V_2O_3 is on the verge of a Mott-Hubbard metal-insulator transition, and, thus, small changes of U have drastic effects. Therefore we will choose U in such a way as to ensure that the LDA+DMFT solution for V_2O_3 is metallic while that for $(V_{0.962}Cr_{0.038})_2O_3$ is insulating. *A posteriori*, we will

compare the adjusted value with those calculated by constrained LDA calculations and those extracted from the experiment.

So far, we did not specify $\hat{H}^0_{\rm LDA}$. In principle, it should contain the valence orbitals, i.e., the oxygen $2p$ orbitals and the five vanadium $3d$ orbitals per atom and, perhaps, even some additional s orbitals. In V_2O_3 the three t_{2g} bands at the Fermi energy are well separated from the other orbitals. Therefore, as a first step we restrict ourselves to the three t_{2g} bands at the Fermi energy which are made up of the corresponding atomic vanadium $3d$ orbitals with some admixtures of oxygen p orbitals. In the case of three degenerate t_{2g} orbitals, which is a good approximation in the case of V_2O_3 since the bandwidths and centers of gravity of the a_{1g} and the doubly-degenerate e^π_g band are very similar, the $\boldsymbol{k}$-integrated Dyson equation simplifies to become an integral over the DOS[15]

$$G_m(\omega) = \int \mathrm{d}\epsilon \frac{N^0_m(\epsilon)}{\omega + \mu - \Sigma_m(\omega) - \epsilon}. \tag{2}$$

Here $G_m(\omega)$, $\Sigma_m(\omega)$, and $N^0_m(\epsilon)$ are the Green function, self energy, and LDA density of states, respectively, for the t_{2g} orbital m. In principle, $N^0_m(\epsilon)$ should contain a double counting correction, which takes into account the fact that parts of the local Coulomb interaction are already included in the LDA. However, this correction results in the same effect for all three orbitals and, hence, only translates into a simple shift of the chemical potential μ. This makes the issue of how to calculate the double counting correction irrelevant for the present purposes. The (shifted) μ has to be controlled according to the vanadium valency, i.e., in such a way that there are two electrons in the three bands at the Fermi energy.

Within DMFT the $\boldsymbol{k}$-integrated Dyson equation (2) has to be solved self-consistently together with a one-site (mean field) problem which is equivalent to an Anderson impurity model with hybridization $\Delta_m(\omega')$ fulfilling[5]

$$[G_m(\omega)]^{-1} + \Sigma_m(\omega) = \omega + \mu - \int_{-\infty}^{\infty} \mathrm{d}\omega' \, \frac{\Delta_m(\omega')}{\omega - \omega'}. \tag{3}$$

The self-consistent solution of the Anderson impurity model given by (3) together with the Dyson equation (2) allows for a realistic investigation of materials with strongly correlated electrons. At small values of U this procedure typically yields a spectrum with a central quasiparticle resonance at the Fermi energy and incoherent Hubbard side bands, while at larger values of U the quasiparticle resonance disappears and a metal-insulator transition occurs. This approach has been successfully applied to a number of transition metal oxides, transition metals, and elemental Pu and Ce[15].

In the present paper, we solve the multi-band Anderson impurity model by QMC[16,5], where by means of the Trotter discretization and Hubbard-Stratonovich transformations the interacting Anderson impurity model is mapped into a sum of non-interacting problems, the sum being performed by the Monte-Carlo technique. We employ a Trotter discretization of $\Delta\tau = 0.25\,\mathrm{eV}^{-1}$ unless noted otherwise and follow Ref. 17 for the Fourier transformation between Matsubara frequencies and imaginary time τ.

To obtain the physically relevant spectral function $A_m(\omega) = -\frac{1}{\pi}\mathrm{Im}G_m(\omega)$ we employ the maximum entropy method[18]. This statistical approach allows one to solve

$$G_m(\tau) = \int_{-\infty}^{\infty} \mathrm{d}\omega \, \frac{e^{\tau(\mu-\omega)}}{1 + e^{\beta(\mu-\omega)}} A_m(\omega) \tag{4}$$

for $A_m(\omega)$, i.e., to analytically continue from imaginary time to real frequencies. The QMC has the advantage of being numerically exact, the main disadvantage being the inability to reach very low temperatures. Indeed, the room temperature calculations of this paper were computationally very expensive, using up to 40 iterations with up to 2×10^5 sweeps and requiring about 2×10^5 hours CPU time. For the implementation of QMC in the context of LDA+DMFT, including flow diagrams, see Ref. 15.

3 Results for V_2O_3

Using the crystal structure of paramagnetic metallic (PM) V_2O_3 and paramagnetic insulating (PI) $(V_{0.962}Cr_{0.038})_2O_3$, respectively, as input we performed LDA+DMFT(QMC) calculations with one a_{1g} and two degenerate e_g^π bands. At $U = 4.5\,\mathrm{eV}$ both crystal structures lead to spectra showing metallic behavior, with a lower Hubbard band between $-2\,\mathrm{eV}$ and $-0.5\,\mathrm{eV}$ (peaked at about $-1\,\mathrm{eV}$), an upper Hubbard band between $1\,\mathrm{eV}$ and $6\,\mathrm{eV}$ and a quasiparticle peak at the Fermi edge. The peak at about $1\,\mathrm{eV}$ is split from the upper t_{2g} Hubbard band due to Hund's rule exchange.

By contrast, at $U = 5.5\,\mathrm{eV}$, both crystal structures lead to spectra showing nearly insulating behavior. The lower Hubbard band is strongly enhanced whereas at the Fermi edge a pseudo-gap is formed. Above the Fermi energy, the two-peak structure is changed only slightly.

Apparently, qualitatively different spectra for the two crystal structures require an intermediate value of U. This is indeed observed at $U = 5.0\,\mathrm{eV}$. Whereas pure V_2O_3 now shows a small peak at the Fermi edge (a residue of the quasiparticle peak obtained at $U = 4.5\,\mathrm{eV}$) and is therefore metallic, the Cr-doped system exhibits a pronounced minimum in the spectrum implying that it is nearly insulating. Due to the rather high temperature at which the QMC simulations were performed ($T = 0.1\,\mathrm{eV} \approx 1160\,\mathrm{K}$) one observes only a smooth *crossover* between the two phases with a metal-like and insulator-like behavior of the respective curves instead of a sharp metal-insulator transition as would be expected for temperatures below the critical point (i.e., for $T < 400\,\mathrm{K}$ in the experiment).

To study V_2O_3 near the metal-insulator transition at experimentally relevant temperatures we performed calculations at $T = 700\,\mathrm{K}$ and $T = 300\,\mathrm{K}$. Since the computational effort is proportional to T^{-3}, those low temperature calculations were computationally very expensive. Fig. 1 shows the results of our calculations at $T = 1160\,\mathrm{K}$, $T = 700\,\mathrm{K}$, and $T = 300\,\mathrm{K}$ for metallic V_2O_3 and at $T = 1160\,\mathrm{K}$ and $T = 700\,\mathrm{K}$ for insulating $(V_{0.962}Cr_{0.038})_2O_3$[19]. In the metallic phase the incoherent features are hardly affected when the temperature is changed, whereas the quasiparticle peak becomes sharper and more pronounced at lower temperatures.

In Fig. 2, the LDA+DMFT results at $300\,\mathrm{K}$ are compared with early photoemission spectra by Schramme[20] and recent high-resolution bulk-sensitive photoemission spectra by Mo *et al.*[21]. The strong difference between the experimental results is now known to be due to the distinct surface sensitivity of the earlier data. In fact, the photoemission data by Mo *et al.*[21] obtained at $h\nu = 700\,\mathrm{eV}$ and $T = 175\,\mathrm{K}$ exhibit, for the first time, a pronounced quasiparticle peak. This is in good qualitative agreement with our low temperature calculations. However, the experimental quasiparticle peak has more spectral weight. We note that while in the theory the peak considerably sharpens with decreasing temperatures, its weight only increases by 11% from 1160K to 300K. The origin for this discrepancy for a system as close to a Mott transition as V_2O_3 is presently not clear.

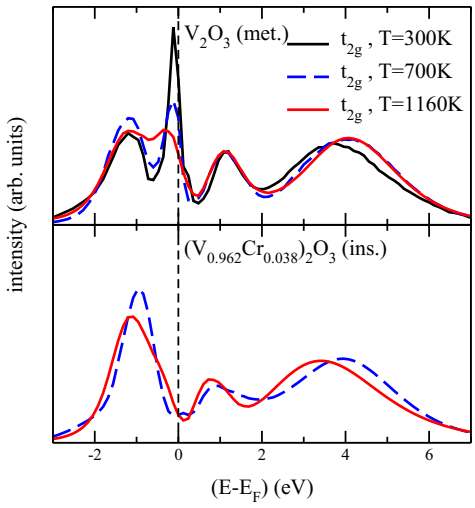

Figure 1. LDA+DMFT(QMC) spectra for paramagnetic insulating $(V_{0.962}Cr_{0.038})_2O_3$ and metallic V_2O_3 at $U = 5$ eV.

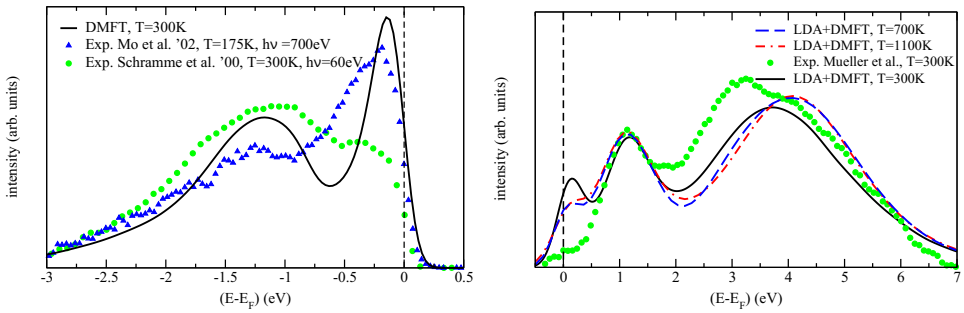

Figure 2. Right: Comparison of LDA+DMFT(QMC) results at $T = 300$ K and $U = 5$ eV with photoemission data by Schramme *et al.*[20] and Mo *et al.*[21] for metallic V_2O_3; Left: Comparison of LDA+DMFT(QMC) results at $U = 5$ eV with X-ray absorption data by Müller *et al.*[22] for metallic V_2O_3

While the comparison with PES data provides important insight into the physics of V_2O_3, more than half of the theoretical spectrum lies above E_F. For this region we compare our results at 1160 K, 700 K, and 300 K with O $1s$ X-ray absorption spectra (XAS) for V_2O_3 at 300 K by Müller *et al.*[22] (see Fig. 2). Since in the XAS-data the Fermi energy is not precisely determined, the data were shifted so that the peaks at 1.1 eV coincide; all curves were normalized to the same area.

The theoretical spectra above E_F are found to be almost independent of temperature. Just above the Fermi energy they all show some structure (i.e., a shoulder at higher temperatures developing into a small peak at low temperatures (300 K)) which is the residue of the quasiparticle peak. Furthermore, at 1.1 eV there is a rather narrow peak, and at about

4.2 eV a broad peak. The latter two structures are parts of the upper Hubbard band which is split due to the Hund's rule coupling J. Hence, the relative position of those two peaks can be expected to depend sensitively on the value of J. A slightly smaller value of J will therefore yield an even better agreement with experiment.

The absence of any quasiparticle weight near E_F in the XAS data is puzzling. This quasiparticle weight is not only present in the theoretical spectra above *and* below E_F, but is also seen in the high resolution PES measurements by Mo *et al.*[21] below E_F.

4 Concluding Remarks

At present, LDA+DMFT is the only available *ab initio* computational technique which is able to treat heavy fermions, f-electron materials and correlated electron systems close to a Mott-Hubbard metal-insulator transition. Using LDA-calculated densities of states for paramagnetic metallic V_2O_3 as well as paramagnetic insulating $(V_{0.962}Cr_{0.038})_2O_3$ as input, we performed DMFT(QMC) calculations at 300 K, 700 K, and 1160 K for various U values. For $U \approx 5$ eV, the calculated spectra show a Mott-Hubbard MIT (or, rather, a sharp crossover).

The 300 K spectrum calculated for metallic V_2O_3 is in good overall agreement with new bulk-sensitive PES measurements[21]. On the other hand, the difference in the quasiparticle weight remains to be explained. The comparison with X-ray absorption measurements shows that our LDA+DMFT(QMC) calculations also give a good description of the spectrum above the Fermi energy.

All calculations described above were performed using the integral over the LDA density of states (Eq. (2)) to obtain the lattice Green function. For a non-cubic system, this procedure is an approximation to the exact LDA+DMFT scheme. In the future we plan to make use of the full Hamiltonian H^0 (Eq. (1)). In this way it will be possible to study the influence of correlation effects on all orbitals including the e_g^σ orbitals and the oxygen states.

The multi-orbital quantum Monte-Carlo simulations used in our LDA+DMFT calculations are computationally very expensive and require powerful computing resources, especially for calculations at experimentally relevant temperatures.

Acknowledgments

We thank J. W. Allen, I. S. Elfimov, M. Feldbacher, S. Horn, A. I. Lichtenstein, A. I. Poteryaev, Th. Pruschke, G. A. Sawatzky and L.H. Tjeng for valuable discussions. This work was supported in part by the Deutsche Forschungsgemeinschaft (DFG) through Sonderforschungsbereich 484, the Emmy Noether program of the DFG (K. H.), the Russian Foundation for Basic Research Grant No. RFFI-01-02-17063 (V. I. A.), the Leibniz-Rechenzentrum, München, and the John von Neumann - Institut für Computing, Jülich. We thank A. Sandvik for making his maximum entropy code available to us.

References

1. For an introductory discussion see G. Kotliar and D. Vollhardt, Physics Today **57**, No. 3 (March), 53 (2004).

2. For a recent review of the electronic correlation problem, see M. Imada, A. Fujimori, and Y. Tokura, Rev. Mod. Phys. **70**, 1039 (1998).
3. N. F. Mott, Rev. Mod. Phys. **40**, 677 (1968); *Metal-Insulator Transitions* (Taylor & Francis, London, 1990).
4. D. B. McWhan, A. Menth, J. P. Remeika, W. F. Brinkman, and T. M. Rice, Phys. Rev. B **7**, 1920 (1973).
5. A. Georges, G. Kotliar, W. Krauth and M. Rozenberg, Rev. Mod. Phys. **68**, 13 (1996).
6. W. Metzner and D. Vollhardt, Phys. Rev. Lett. **62**, 324 (1989).
7. A. Georges and G. Kotliar, Phys. Rev. B **45**, 6479 (1992).
8. M. Jarrell, Phys. Rev. Lett. **69**, 168 (1992).
9. One limitation of QMC is that it is very difficult to deal with the spin-flip term of the Hund's rule coupling because of a "minus-sign problem" which arises in a Hubbard-Stratonovich decoupling of this spin-flip term, see K. Held, Ph.D. thesis, Universität Augsburg 1999 (Shaker Verlag, Aachen, 1999).
10. V. I. Anisimov, A. I. Poteryaev, M. A. Korotin, A. O. Anokhin, and G. Kotliar, J. Phys.: Cond. Matt. **9**, 7359 (1997); A. I. Lichtenstein and M. I. Katsnelson, Phys. Rev. B **57**, 6884 (1998).
11. I. A. Nekrasov, K. Held, N. Blümer, V. I. Anisimov, and D. Vollhardt, Euro. Phys. J. B **18**, 55 (2000).
12. V. I. Anisimov, D. E. Kondakov, A. V. Kozhevnikov, I. A. Nekrasov, Z. V. Pchelkina, J. W. Allen, S.-K. Mo, H.-D. Kim, P. Metcalf, S. Suga, A. Sekiyama, G. Keller, I. Leonov, X. Ren, and D. Vollhardt, Phys. Rev. B **71**, 125119 (2005).
13. L. Hedin and B. Lundqvist, J. Phys. C: Solid State Phys. **4**, 2064 (1971); U. von Barth and L. Hedin, J. Phys. C: Solid State Phys. **5**, 1629 (1972); D. M. Ceperley and B. J. Alder, Phys. Rev. Lett. 45, 566 (1980).
14. R. Bulla, T. A. Costi, D. Vollhardt, Phys. Rev. B **64**, 045103 (2001).
15. For reviews see K. Held, I. A. Nekrasov, G. Keller, V. Eyert, N. Blümer, A.K. McMahan, R.T. Scalettar, Th. Pruschke, V.I. Anisimov und D. Vollhardt, "Realistic investigations of correlated electron systems with LDA+DMFT", Psi-k Newsletter #56, 65 (2003) `http://psi-k.dl.ac.uk/newsletters/News_56/Highlight_56.pdf`; A. I. Lichtenstein, M. I. Katsnelson, G. Kotliar, *Electron Correlations and Materials Properties 2*, 2nd ed., A. Gonis, N. Kioussis, M. Ciftan, ed. Kluwer Academic/Plenum, New York (2003), available at `http://arXiv.org/abs/cond-mat/0211076`.
16. J. E. Hirsch and R. M. Fye, Phys. Rev. Lett. **56**, 2521 (1986).
17. M. Ulmke, V. Janiš, and D. Vollhardt, Phys. Rev. B **51**, 10411 (1995).
18. M. Jarrell and J. E. Gubernatis, Physics Reports **269**, 133 (1996).
19. In spite of extensive computations the calculations at 300 K in the insulating phase did not yield sufficiently converged results and are therefore not shown in Fig. 1.
20. M. Schramme, Ph.D. thesis, Universität Augsburg, 2000; M. Schramme *et al.* (unpublished).
21. S.-K. Mo, J. D. Denlinger, H.-D. Kim, J.-H. Park, J. W. Allen, A. Sekiyama, A. Yamasaki, K. Kadono, S. Suga, Y. Saitoh, T. Muro, P. Metcalf, G. Keller, K. Held, V. Eyert, V. I. Anisimov, D. Vollhardt, Phys. Rev. Lett. **90**, 186403 (2003).
22. O. Müller, J.-P. Urbach, E. Goering, T. Weber, R. Barth, H. Schuler, M. Klemm, S. Horn, and M. L. denBoer Phys. Rev. B **56**, 15056 (1997).